

Characterization of different forms of chalcopyrite disease through fractal analysis

Shubham Tripathi^{1,*} and Sushil K. Singh²

¹Department of Geology, University of Delhi, Delhi 110 007, India

²Department of Physics, SGTB Khalsa College, University of Delhi, Delhi 110 007, India

Complex shapes that form by natural processes are often difficult to explain using non-Euclidean geometry. Chalcopyrite disease (CD) formation, a replacement texture, demonstrates a nonlinear-fractal geometry. CD samples from three polymetallic deposits were chosen for fractal analysis. CD did not show a fractal value specific to mineralized deposits. However, fractal analysis showed consistent values for a similar form of CD, thus setting a quantitative relationship between varied forms of CD and their condition of formation. The mean fractal dimension calculated for each study area displayed a positive correlation with the peak metamorphic grade of the respective deposit. The statistical analysis (ANOVA) of fractal dimension data further delineated the differences among the three study areas.

Keywords: Box counting method, chalcopyrite disease, fractal dimension, replacement texture, statistical analysis.

CHALCOPYRITE blebs in different forms on sphalerite grains are a common textural feature observed in mineral deposits. This feature has been extensively studied because of the unique display of different shapes of chalcopyrite, variation of sphalerite composition associated with this texture and its utility in establishing paragenetic relationship between ore minerals. Several theories were put forward to explain the chalcopyrite–sphalerite texture, a widely debated topic in ore microscopy, since its initial interpretation as exsolved product from sphalerite^{1–4}. Nakano⁵ first suggested that chalcopyrite blebs and dots in Kuroko type ores resulted from replacement of zinc sulphide. Barton⁶ introduced the term ‘chalcopyrite disease’ (CD) for this sphalerite–chalcopyrite relationship. Later studies proposed replacement to explain such texture by reaction of iron from sphalerite with copper ions transported in hydrothermal solution^{7,8}. Experimental studies on the Cu–Fe–Zn–S system also supported the concept that chalcopyrite blebs, dots and dust may be produced by replacement processes^{9–14}. Recent experimental studies have shown that metamorphism-induced partial melting of sulphide ores facilitates the formation

of CD by producing a Cu-enriched but S-deficient melt phase and Fe- and S-enriched sphalerite. It was observed that for CD to develop, the Cu-enriched solidified melt must exist in close contact with the Fe-enriched sphalerite^{15,16}.

Bente and Doering^{17,18} focused on experimental simulation of CD formation through solid-state diffusion studies. They showed that the different diseased forms emerge by metal inter-diffusion depending on the solid solubilities, temperature, time, sulphur fugacity, oxygen fugacity, water pressure, Cu:Fe ratio in the diffusion source and Fe content in the sphalerite receptor. They proposed the term ‘diffusion-induced segregation’ (DIS) instead of ‘disease’. They also concluded that the grain size, form and orientation of the DIS bodies also depend on the annealing temperature, annealing time and defects of the sphalerite crystal. Extensive studies have been done on the annealing behaviour of ore minerals. Some workers prefer to use the term static recrystallization instead of annealing. We would still use the term ‘annealing’ in this study, considering its widespread acceptability by ore petrologists. Also, many deposits undergo post-recrystallization deformation, overprinting their features on annealed samples. The complexity due to all these metamorphic events on CD grain boundaries has not yet been quantified. One possible way to do this would be through fractal study.

Fractal, a relatively new mathematical concept, helps quantify and explain the complex shapes of natural objects. Mandelbrot¹⁹ coined the word ‘fractal’ to explain the concept of self-similarity present in a number of objects that cannot be explained by Euclidean geometry. Fractal-like structures may be created wherever nonlinear dynamical mechanisms are at work. Such mechanisms may create inhomogeneity over a large range of physical space. Several studies have also been conducted on the fractal nature of grain boundaries of two different substances. Experiments and simulation studies have shown that grain boundaries during diffusion-induced reactions, such as the ones proposed for the formation of CD, develop fractal ‘fingering’ due to growth instability which could accelerate the interfacial motion, resulting in increase in the complexity of the boundaries²⁰, this may be the reason for the non-Euclidean behaviour (fractal) of the grain boundaries. The concept of fractals has been

*For correspondence. (e-mail: stripathi@live.in)

extensively used in geological studies, as well as in the discipline of economic geology^{19,21–23}.

Mineral textures are a reflection of their conditions of formation. Various approaches are used for both quantitative and qualitative textural analysis. As mentioned earlier, fractals remain a useful method for quantitative characterization. Nevertheless, establishing a relationship between fractal dimension (FD) (a ratio providing a statistical index of complexity) and various geological conditions that control textural pattern remains a challenge. Fractal studies have mostly been limited to silicate minerals^{24–29}. Not much work has been done on the fractal nature of sulphides and specifically their textures^{30–32}, in spite of the fact that they reveal a lot of information about the geological setting and conditions of formation of a mineral deposit. To our knowledge, the complex nature of CD has also not been studied using the technique of fractal analysis. The experimental constraints for the formation of complex shapes of CD as explained by Bente and Doering¹⁸, has little bearing on natural samples. Thus the present work tests the veracity of this experimental finding using natural samples, and attempt to quantify the complexity of the shapes of CD using fractals.

Fractals and box counting method

Fractal objects are identified by their unique attribute that when magnified reveals ever finer features, which are similar to the larger features, termed as ‘self-similarity’. In contrast, a non-fractal object when magnified reveals no new feature. Furthermore, for a non-fractal object there exists a characteristic scale (resolution) at which the correct values of length, area and volume can be determined. Fractal objects have no such characteristic scale and therefore values of length, area and volume are resolution-dependent. We do not get a unique value of the length, area or volume of a fractal object if the measurements are made at different resolutions. Another important characteristic of fractal objects is scaling. They are found to have features over a broad range of sizes. FD gives a quantitative measure of self-similarity and scaling. For some special object the fractal index can be based on length (like the perimeter) measurements at different scales. For a highly self-similar object, the fractal index can be based on finding the resolutions at which the scaled object matches the object itself.

Objects that are self-similar and display non-integer dimension are referred by the term ‘capacity dimension’, which is a generalization of the self-similarity dimension. Box counting method remains the most useful technique to calculate the capacity dimension. This method relates a measured property A of the object to the resolution s at which it is being measured. The measured value $A(s')$ at a scale s' is \times times $A(s)$ (that measured at scale s). Such a scaling law predicts a power law relationship between the measured value $A(s)$ and the scale s .

$$A(s) = \beta s^{D_B},$$

where β is a constant and D_B is the box dimension of the object.

A plot of log of the measured quantity versus log of the resolution used to make the measurement is a straight line and is characteristic of fractal objects. The box dimension is then defined as the slope of the log–log plot between the number of boxes intercepted by the object and the inverse of the size of the boxes.

$$\frac{\log N(s)}{1/s}.$$

The values of box dimension D_B should be between 1 and 2 in 2D space. This means that when using $D_B \rightarrow 1$, it implies that the subject under study is more irregular in shape, while when $D_B \rightarrow 2$, it is organized and gravitates towards a round shape²⁸. The fractal values of CD vary between 1 and 2 because the area represented in the plane space is in fact a closed curve like a 2D object, and thus warrants the same conclusion of its box dimension D_B (Figure 1). In the present study, we have taken area of the blebs as the measured property $A(s)$. We expect that the individual blebs would also reveal fractal self-similarity if they are analysed through fractal fingerprinting. Because of self-similarity, features at one spatial resolution are related to those at another spatial resolution. Smaller features are therefore copies of larger features.

Background of samples studied

Twelve samples from the three Pb–Zn deposits/prospects in India, Ambaji–Deri, Rajpura–Dariba and Imalia were chosen. The samples from the three deposits are useful in the context of this study because they show CD. These samples are representative of the different forms in which CD is present in these areas (Figure 2).

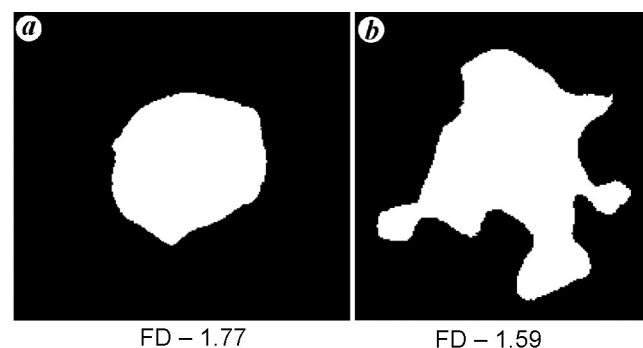


Figure 1. Variation of fractal dimension (FD) of a single grain of chalcopyrite disease (CD) samples from the study areas. (a) Ambaji–Deri and (b) Imalia. Chalcopyrite grain from Ambaji–Deri has higher FD (tending towards 2) and a more regular shape, whereas chalcopyrite grain from Imalia has lower FD and irregular shape.

Massive, stratiform, zinc–lead–copper ores occur at Ambaji and Deri, located 8 km apart, in the states of Gujarat and Rajasthan respectively. The ores are concentrated in lensoid bodies and patches of metamorphosed magnesian and calc-magnesian rocks, such as cordierite–anthophyllite–chlorite rocks, quartz–chlorite–tremolite schists and diopside–forsterite marble, enclosed within argillaceous and arenaceous metasediments or ortho-amphibolites. The rocks belong to the lower part of the Ajabgarh group of the Precambrian Delhi Supergroup³³. The host rocks and ores were subjected to an earlier low-grade regional metamorphism under greenschist facies conditions and a superimposed hornblende hornfels facies thermal metamorphism apparently related to the intrusion of granite and alkali syenite plutons at Ambaji and Deri respectively. The main ore minerals present in the deposit are sphalerite, galena, chalcopyrite, pyrite and magnetite³⁴.

Rajpura–Dariba, a polymetallic deposit, lies within the Rajsamand district in Rajasthan. Host rocks for the mineralization comprise recrystallized siliceous dolostone, graphite mica schists and carbonaceous schist and carbonaceous chert within the Bhilwara belt. The ore along with the host rock was isofacially metamorphosed, and the timing of metamorphism has been envisaged at 1.6 Ga (ref. 35). The important sulphide minerals in this deposit consist of sphalerite, galena, pyrrhotite, pyrite and chalcopyrite. Ore bodies are stratabound, stratiform as well as stratified into ore rhythmites, and considered to be a SEDEX-type deposit.

Imalia, a polymetallic prospect, is located in Katni district, Madhya Pradesh. It lies in the western part of the Mahakoshal belt in Central India. Imalia comprises a sequence of metasediments represented by shale, slate

and phyllite interbedded with dolomite and limestone, quartzite and conglomerates of the Agori Formation³⁶. The calculated Pb–Pb isotope date for this prospect is late Paleoproterozoic. The metasediments are intruded by dykes of quartz porphyry and basic rocks. Mineralization is confined within the massive and bedded dolomites, and comprises pyrite, arsenopyrite, galena, sphalerite, chalcopyrite, tetrahedrite, magnetite, electrum and a host of rare phases³⁷.

Methodology

The digital colour photographs of the diseased chalcopyrite samples were taken using an image analyser microscope (Lieca DMRX, Germany) under crossed polarized beam. For consistency, all the images were taken at the same scale of 50× magnification. To incorporate all forms of CD present in each of the samples, three representative images taken at different spots were chosen for fractal analysis. The images were also taken at 20× at the same position to check if the blebs display self-similar characteristics at different scales. The photographs for fractal analysis were then converted into black-and-white binary images, where against the white background, black patches of chalcopyrite blebs could be used for fractal analysis. This was done in MATLAB. Due care was taken to make sure that the grain boundary shapes are in no way compromised during the conversion process. Also, other sulphides that were closely associated with the chalcopyrite diseased portion were duly cropped. Peternell and Kruhl³⁸ studied the efficacy of digital images for fractal analysis and reported that automated recorded patterns of mineral distribution were suitable for box counting. They observed that even when automatically digitized grain boundaries are not precise, the FD results are not affected and quantification of rock fabric is possible without loss of accuracy. The fractal analysis was done in MATLAB. The images were again rechecked for FD using Fraclac software, and the results were consistent in both the analysis. Fractal analysis was done using box counting method, which calculates FD by plotting on a log–log diagram, the number of boxes $N(r)$ intercepted and the scale used to make a unit box (r ; Figure 3). During box counting, the range of box sizes, r , has to be carefully selected, the reason being that the box size cannot be smaller than the smallest chalcopyrite bleb (i.e. in the case of an image, it is the size of the pixel). Otherwise, the number of counted boxes (N) does not change with box size smaller than the pixel size and FD would be zero. Whereas if it is equal to the size of the smallest object building up the pattern (one pixel), then FD would tend to 1 (ref. 39). Therefore, the lowest limit of the unit size of the box should be above one pixel, and for the present analysis it was fixed at two pixels. This lower limit was chosen as there should be a limit for decreasing the size of boxes.

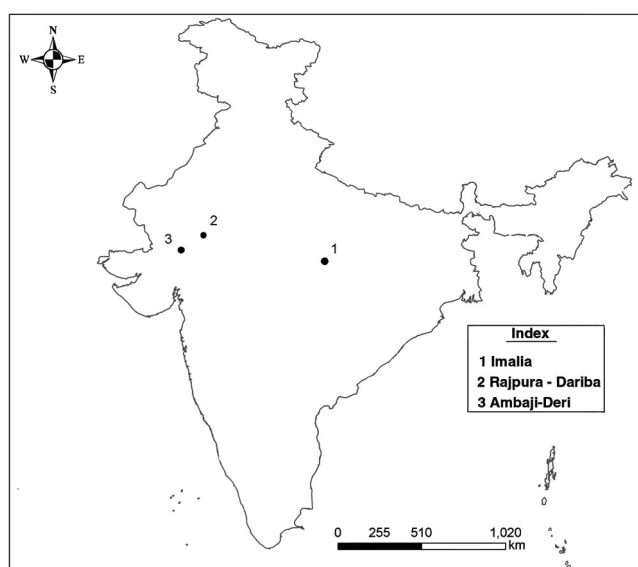


Figure 2. Geological map of India showing location of deposits/prospects under study.

After calculating FD of samples from three different locations, the data were further statistically evaluated to understand the differences between the three deposits, and if they correlate with the different conditions of formation. For statistical analysis of such data, ANOVA has been a useful tool. Samples displaying normal distribution alone can be used for ANOVA. To check whether ANOVA could be used in the present case, Shapiro–Wilk test was performed prior to the analysis. To acquire detailed information from the ANOVA test results, Tukey HSD analysis was done. The test allowed multiple comparisons among different study areas between and within the groups. The statistical analysis was done in MATLAB.

Results

As discussed in the previous section, images displaying FD values between 1 and 2 measured in a two-dimensional space are fractal in nature. In the CD photomicrographs, the blebs are found to be present in different sizes at 2–3 iterations, revealing new details at different scales indicating their fractal nature. Therefore, fractal dimension D can be used as one of the features to represent or classify irregular (completely natural)-shaped objects. These objects are unlikely to have a characteristic value of length,

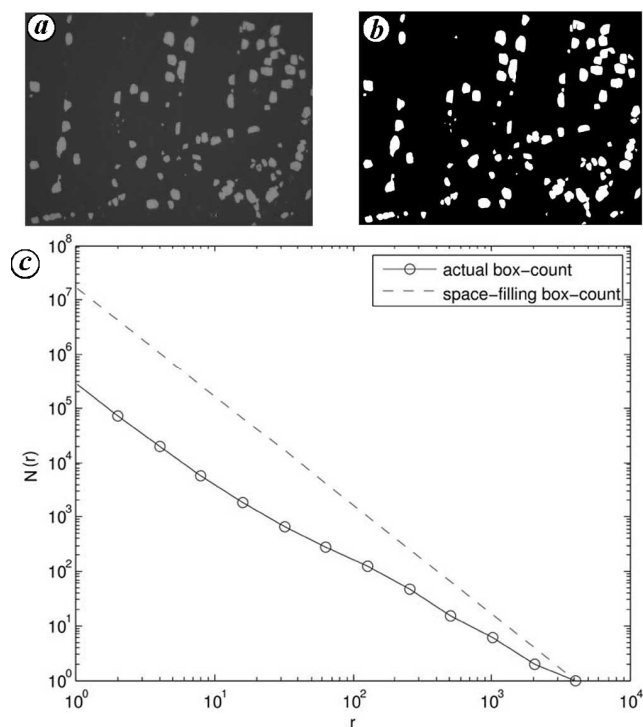


Figure 3. Image processing. *a*, Photomicrograph of CD. *b*, Binary image of the same, with white patches of chalcopyrite blebs against a black background. *c*, Calculated FD values shown on a log–log plot, where r represents unit box size for the image in pixels, and $N(r)$ is the number of boxes occupied by the chalcopyrite grains.

area or volume independent of the scale. Also, scale measurement is an important issue in extracting meaningful geological information from rock textures across spatial scales. The scale independence of fractal dimension (FD) derives its basis from the assumption that the same processes control the observed patterns from the smallest to the largest scale. For CD to be fractal in nature and display self-similar characteristics, its FD has to be constant over a finite range of measurement scales. The results on the contrary showed differences at 20 \times and 50 \times magnification. The reason is that at low magnification very small CD blebs, lower than two pixels, were not identified by the program. However, at higher magnification the same blebs were included in the calculation, resulting in variation of FD values. However, when FD of an individual bleb at both magnifications was calculated, the results were identical, conforming the scale-independent nature of CD. Four representative samples each from the three deposits chosen for the study had different forms of CD ranging from lamellar, ellipsoidal, polyhedral, blebs and dusty chalcopyrite in sphalerite. The FD of these different textures was obtained by box counting; Table 1 shows the results. A brief textural description of each sample and the calculated FD values reveals lot of pertinent information.

Different forms of CD from the samples of Ambaji and Deri deposits have a mean FD of 1.38. Highest FD was calculated for samples AD1 and AD2 of Ambaji that generally display uniformly distributed coarse-to fine-grained blebs and ellipsoidal chalcopyrite in sphalerite (Figure 4 *a* and *b*, top). At places they followed the direction of annealing twins and cracks in sphalerite. In sample AD2, the chalcopyrite grains at places were bent and elongated possibly due to later deformation. Sample AD3 too had predominantly blebs and ellipsoidal grains, but they were smaller and not regularly arranged like the previous two samples. Lamellar texture was also observed at places (Figure 4 *c*, top). Sample AD4 had CD showing lamellar texture, where chalcopyrite filled the cracks of the sphalerite grains (Figure 4 *d*, top), along with scattered chalcopyrite blebs and polyhedral grains. These samples from Deri had lower FD compared to samples showing coarse blebs and ellipsoidal grains.

Not much variation was observed in FD of the Rajpura–Dariba samples, that had a mean value of 1.34. Samples RD1 and RD2 both showed bimodal grain distribution: medium-sized blebs and large polyhedral grains on a sphalerite mass (Figure 4 *a* and *b*, middle). Lamellar texture was also present in both the samples along the twin direction, and few scattered blebs. Samples RD3 and RD4 had CD as randomly distributed blebs, polyhedral, ellipsoidal grains and chalcopyrite dust (Figure 4 *c* and *d*, middle). CD was also identified in the form of irregular chalcopyrite grains filling the sphalerite cracks.

At Imalia, CD was mainly present as randomly distributed, medium-sized blebs, polyhedral grains to dusty

Table 1. Results of fractal dimension of samples from three mineral deposits/prospects

Deposit/prospect	Sample no.	FD	Magnification	Texture
Ambaji Deri	AD1a	1.45	50×	Coarse blebs
Ambaji Deri	AD1b	1.47	50×	Coarse blebs, few elliptical grains
Ambaji Deri	AD1c	1.52	50×	Coarse blebs alinged along twin direction
Ambaji Deri	AD1c1	1.40	20×	Coarse blebs alinged along twin direction
Ambaji Deri	AD2a	1.55	50×	Coarse blebs, few blebs aligned twin direction
Ambaji Deri	AD2a1	1.41	20×	Coarse blebs, few blebs aligned twin direction
Ambaji Deri	AD2b	1.41	50×	Coarse blebs, few of them aligned along twin direction
Ambaji Deri	AD2c	1.40	50×	Coarse blebs alinged twin along direction
Ambaji Deri	AD3a	1.33	50×	Blebs and elliptical grains
Ambaji Deri	AD3b	1.25	50×	Blebs and elliptical grains
Ambaji Deri	AD3c	1.37	50×	Blebs and Lamellar grains
Ambaji Deri	AD4a	1.29	50×	Medium sized blebs, polyhedral grains
Ambaji Deri	AD4b	1.26	50×	Blebs, chalcopyrite filling cracks of sphalerite
Ambaji Deri	AD4c	1.22	50×	Medium sized blebs, polyhedral grains
Rajpura–Dariba	RD1a	1.40	50×	Bimodal distribution – blebs and coarse polyhedral grain
Rajpura–Dariba	RD1b	1.32	50×	Bimodal distribution – blebs and coarse polyhedral
Rajpura–Dariba	RD1c	1.18	50×	Blebs, lamellar grains aligned along the twin
Rajpura–Dariba	RD2a	1.34	50×	Bimodal distribution – blebs and polyhedral chalcopyrite grain
Rajpura–Dariba	RD2b	1.47	50×	Coarse polyhedral grains, lameller texture along twin direction
Rajpura–Dariba	RD2c	1.28	50×	Blebs and lameller texture
Rajpura–Dariba	RD3a	1.40	50×	Scattered blebs, ellipsoidal grains, dust
Rajpura–Dariba	RD3b	1.32	50×	Polyhedral grains, ellipsoidal grains fill sphalerite cracks
Rajpura–Dariba	RD3c	1.42	50×	Scattered belbs and coarse polyhedral grains
Rajpura–Dariba	RD4a	1.37	50×	Lameller texture
Rajpura–Dariba	RD4b	1.46	50×	Scattered polyhedral grains
Rajpura–Dariba	RD4b1	1.33	20×	Scattered polyhedral grains
Rajpura–Dariba	RD4c	1.18	50×	Irregular grains fillings sphalerite cracks
Imalia	IM1a	1.22	50×	Scattered blebs, polyhedral grains
Imalia	IM1b	1.16	50×	Scattered blebs
Imalia	IM1c	1.28	50×	Scattered blebs
Imalia	IM2a	1.12	50×	Scattered blebs, few polyhedral grains
Imalia	IM2b	1.32	50×	Scattered blebs, they colasce at the margins as irregular grains
Imalia	IM2c	1.17	50×	Scattered blebs, ellipsoidal, polyhedral grains
Imalia	IM3a	1.19	50×	Scattered Blebs, ellipsoidal, polyhedral grains
Imalia	IM3a1	1.08	20×	Scattered blebs, polyhedral grains
Imalia	IM3b	1.13	50×	Scattered Blebs, ellipsoidal, polyhedral grains
Imalia	IM3c	1.02	50×	Scattered blebs
Imalia	IM4a	1.15	50×	Scattered blebs and dusty chalcopyrite
Imalia	IM4b	1.25	50×	Scattered dusty chalcopyrite, blebs, polyhedral grains
Imalia	IM4c	1.18	50×	Scattered dusty chalcopyrite, blebs, polyhedral grains

chalcopyrite (Figure 4 *a*, bottom). In sample IM2, medium-sized chalcopyrite grains had irregular form, mainly at the margins of the sphalerite grain, probably due to coalescing of smaller grains during the later episode of mild metamorphism (Figure 4 *b*, bottom). The mean FD of samples from Imalia was 1.17, the lowest in samples from all the three studied deposits. The chalcopyrite dust mostly present in few samples from Imalia is often too small to mark the grain boundaries; therefore, it was mostly excluded from fractal analysis. However, when the individual dust grains were enlarged to draw an approximate outline of the grain shape, and the FD was calculated, the result tended towards 1, indicating their irregular form, a common feature of the grain shape after nucleation. Most samples from Imalia seem to have not undergone much change after their formation, the probable reason why they display scattered CD and lower FD.

Nature and conditions of formation of CD among different areas of study have been objectively shown using ANOVA. The Shapiro–Wilk test was performed earlier to check whether the analysed FD data could be used for ANOVA. The results of the test, Ambaji Deri (AD) ($w = 0.93$), Rajpura–Dariba (RD) ($W = 0.96$) and Imalia (IM) ($W = 0.98$) confirm their normal distribution; hence, ANOVA could be used here. The P -value calculated using ANOVA was $0.0002 > 0.05$. Thus we can reject the null hypothesis and safely conclude that the three study areas are significantly different from each other on the basis of their FD data. However, ANOVA does not identify which group is distinct from the other groups. To acquire detailed information from these results, Tukey HSD was performed. This test does multiple comparisons between the deposits under study to identify their statistical variation. The tabular output of Tukey HSD contained

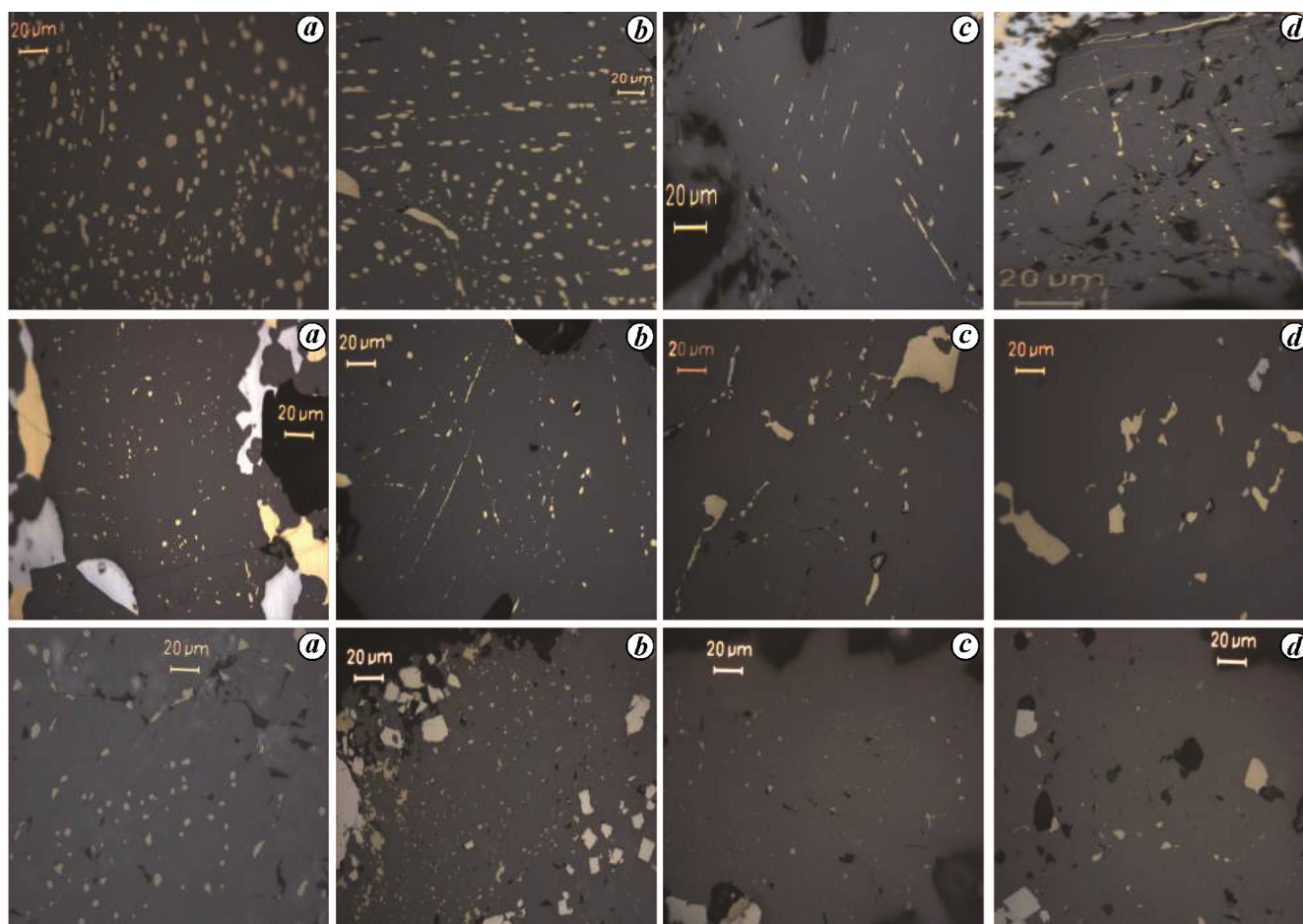


Figure 4. Different forms of CD present in the studied areas. (Top) Ambaji-Deri, (a) Regular arranged coarse blebs, and elliptical grains (b) Coarse blebs and elliptical grains, few aligned along the twin boundaries and also bend due to later deformation, (c) Lamellar chalcocopyrite along the (111) octahedral cleavages of spherulite, few scattered blebs, (d) Chalcocopyrite as scattered blebs and also filling the cracks in the spherulite mass. (Middle) Rajpura-Dariba, (a) Polyhedral chalcocopyrite grains along with randomly distributed blebs, coarse grained galena also visible (b) chalcocopyrite lamellae following the twin boundaries and randomly distributed blebs, (c, d) Polyhedral grains and blebs in spherulite. (Bottom) Imalia, (a) Scattered blebs in the sphaletite mass. (b) Chalcocopyrite blebs that have colapsed at the margins to form bigger grains with rugged grain boundaries; equant arsenopyrite grains are also visible. (c, d) Blebs and dusty chalcocopyrite in spherulite.

P-value of differences between deposits, which are graphically represented in Figure 5 for ease of interpretation.

As evident in Figure 5, only the confidence interval for RD-AD contains 0, whereas the confidence interval of comparison between IM-AD and IM-RD does not include 0. This means that the fractal nature of CD in the samples of Imalia Pb-Zn prospect is significantly distinct when compared separately with the other two deposits, implying their contrasting geological conditions of formation for CD. However, the Tukey HSD comparison between Ambaji-Deri and Rajpura-Dariba deposits indicates only a slight difference in their conditions of formation of CD.

Discussion

The inter-variation in FD results as shown from statistical analysis should have a relation with the complex physico-

chemical environment that conditioned Cu diffusion in spherulite and later metamorphic events. Bente and Doering^{17,18} noted the precise conditions for formation of different forms of CD by experimental recreation of the disease. Those experimental conditions found great semblance in the formation of CD in the studied deposits. For instance, at Ambaji-Deri predominant CD texture were regularly arranged coarse blebs of chalcocopyrite aligned along the crystallographic direction. In the experimental study such texture was produced at high temperature between 500°C and 700°C, at high fS_2 and long period of annealing. Barton and Bethke⁷ maintain that this is not a primary feature, rather a secondary texture formed during metamorphic events. Govindarao *et al.*¹⁵ explain it to be nonstoichiometry-driven diffusion of Cu as the mechanism and sulphide partial melting as the principal reason behind the development of CD in spherulite. Coarse blebs in the experiments by Bente and Doering¹⁸ were generated in the monocrystalline part of spherulite, while the lamellar

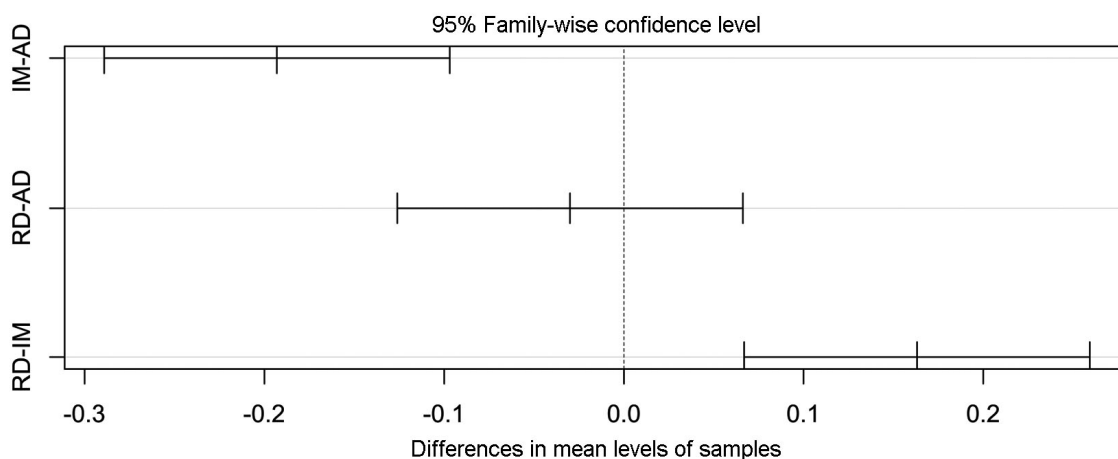


Figure 5. Graphical representation of Tukey HSD results. Dotted vertical line is the mean. Comparison between FD of two deposits is shown by horizontal line. AD, Ambaji–Deri; RD, Rajpura–Dariba; IM, Imalia.

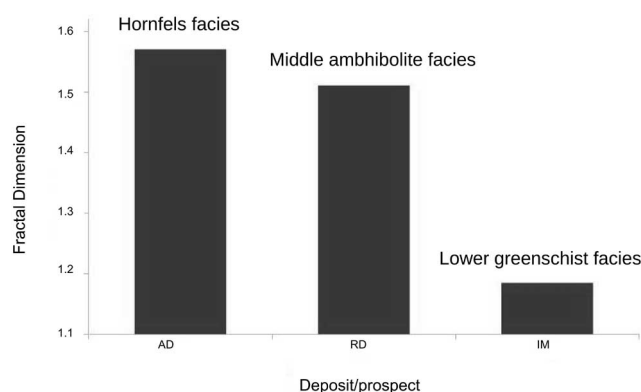


Figure 6. Graph showing mean FD values of the three study areas and peak metamorphic grade.

form was produced along the twin planes of sphalerite. The Fe content in these experiments was $>2\text{--}3$ mol% FeS in sphalerite, an important prerequisite for initiation of metal inter-diffusion, even if other parameters for the reaction were met. At Ambaji–Deri, similar conditions of formation prevailed. The Fe content in sphalerite was above the threshold limit for replacement reaction. Similar to the experimental results, at Ambaji–Deri the sphalerite mineralization possibly occurred at lower sulphur fugacity and later the Cu-bearing source diffused copper into sphalerite at increased sulphur fugacity. Etching of sphalerite containing chalcopyrite grains revealed coherent annealing twins. These were deformed at places, suggesting that deformation outlasted grain growth⁴⁰. The peak temperature of late-stage thermal metamorphic event at Ambaji–Deri was calculated to be at $\sim 550^\circ\text{C}$, and the sulphides have hornfelsic fabric^{34,41}. During annealing the grains try to decrease their surface energy, and tend to have idiomorphic shape as it is most stable and has lower surface energy. This is also reflected in the

fractal results. The regularly arranged coarse blebs at Ambaji–Deri recorded FD values as high as 1.56, where chalcopyrite expanded in size due to annealing at higher temperature for a longer period of time. Li *et al.*⁴² have shown experimentally that as the duration of the annealing time increases, FD tends to show higher values in 2D space. This means they are more organized and tend towards less-strained rounded shapes. The CD that formed in the inhomogeneous part of sphalerite with cracks and fractures did not have the same space to adjust its grain boundaries during annealing; therefore, the lower fractal values are relatively low. Sulphides at Ambaji–Deri also witnessed later mild cataclastic deformation that probably increased the complexity of CD texture. This may be the reason for the presence of deformed annealing twins at places, an indication of deformation outlasting annealing. The presence of elliptical grains in regularly arranged coarse blebs is also the signature of this cataclastic event.

At Rajpura–Dariba the CD ranges from large polyhedral grains, to lamellar form and chalcopyrite dust in sphalerite. Statistical analysis of their fractal data indicates that they are different from those of the Imalia prospect, and closer in conditions of formation with Ambaji–Deri, but not the same. Bente and Doering¹⁸ recreated the textures similar to RD at a temperature range of $450\text{--}500^\circ\text{C}$, where at high fS_2 (sulphur fugacity) worm-like and dusty chalcopyrite was produced. These CD samples when kept at longer annealing times at these temperatures led to the coarsening of grains, and a few formed polyhedral grains. Also in the twinned and fractured part of the sphalerite, chalcopyrite lamellae were formed with crystallographic orientation. The Fe content in sphalerite at Rajpura–Dariba was at ~ 7 mol% FeS, sufficient for replacement reaction to begin. The deposit witnessed isofacial metamorphism of ore-host rocks under conditions of middle amphibolite facies at mean temperature of 540°C

(refs 43–46), consistent with the experimental results. More recent work at Rajpura–Dariba points toward a diffusion of Cu-enriched solidified melt in close contact with the Fe-enriched nonstoichiometric sphalerite that produced chalcopyrite blebs giving rise to CD^{15,16}. In the deposit, the mean FD of 1.34 indicates more organized and regular shapes of chalcopyrite grains, although there is variation within the samples of the deposit depending on the form of CD present. When the FD of individual polyhedral grains was calculated from the samples showing bimodal distribution of CD, the dimension was much larger than the cumulative FD of the whole image. Even the chalcopyrite blebs present in those samples had a more compact shape and tended toward roundness as shown by their FD values. These patterns of chalcopyrite may be due to late partial annealing phenomenon observed in the Rajpura–Dariba ores⁴⁴.

At Imalia, the sphalerite samples display CD mainly in the form of medium to dusty chalcopyrite grains randomly scattered in the host mineral. The mean FD calculated was the least and as discussed earlier, statistical analysis too identified it as different from the other two studied deposits. Mineralization at Imalia occurred at a relatively low temperature of <300°C, and the prospect underwent lower greenschist facies metamorphism. The experiment by Bente and Doering^{17,18} did not cover the formation of CD under these lower temperature conditions. However, as chalcopyrite has a heterovalent nature, it can replace sphalerite even at lower temperatures. Imalia sphalerite samples had a low amount of Fe ranging from 0.6 to 2.3 mol FeS%, less than even the threshold limit of Fe required to allow solid-state diffusion to form CD. Chalcopyrite disease has been reported in Fe-poor sphalerite from many deposits worldwide^{47,48}. One possibility of the generation of CD by DIS would be that the copper-rich overprinting hydrothermal fluids are rich in iron. Very slow diffusion of iron in sphalerite as shown by Mizuta¹¹, goes against this argument. However, his experiments ranged from 500°C to 900°C, and the equation for diffusion must be extrapolated to the 200–300°C range of interest here, raising uncertainty on the conclusion. Another possibility would be co-precipitation of chalcopyrite and sphalerite, where epitaxial nucleation of chalcopyrite grains takes place on the growing surface of sphalerite¹². At Imalia, sphalerite that displays CD is formed at the initial phase of mineralization. The sphalerite does not show deformation twins and other textures that would indicate that it underwent significant deformation and annealing³⁷. The grains are mostly scattered, medium-sized blebs to dusty chalcopyrite. The CD at Imalia formed either by replacement or co-precipitation was initially rapid like in the other deposits due to availability of Fe and Cu in the system forming scattered chalcopyrite grains in sphalerite. Other studies have shown that FD of material during nucleation stage has lower value⁴². This process must have continued till the availa-

bility of both ions and also fulfilling the other geochemical conditions. Unlike the other two deposits, sulphides at Imalia underwent only mild greenschist metamorphism and low temperature annealing for a short duration³⁷. The dusty chalcopyrite grains at places have diffused to the adjacent grain in order to decrease their free surface energy with the help of mild annealing that the ores witnessed, but it was not enough for the coalescing grains to fully reduce their strain energy and increase their size, although localized exceptions at places are observed. Mostly chalcopyrite are dispersed and irregular in shape. This may be one of the main reasons why CD in Imalia samples is more complex and displays lower FD value tending towards 1.

As observed, different forms of CD were present in all three deposits/prospects, although few forms were dominant in one deposit compared to the others. The effects of metamorphism are distinct on the contrasting FD values of all the three study areas. Interestingly, the mean FD graph agreed well with the recorded peak metamorphic grade of these deposits (Figure 6). CD from Imalia had lowest mean FD that witnessed lower greenschist facies peak metamorphism, while Ambaji–Deri recorded the highest FD that witnessed peak hornfels facies metamorphism. This raises a question whether there exists a positive correlation between grade of metamorphism and FD. Metamorphic intensity undoubtedly has a direct impact on the size and complexity of grain boundaries of chalcopyrite, as metamorphism generally masks the previous signatures. However, it may not be the sole controlling factor. New experimental findings show that CD formed due to partial melting, where Cu-enriched, solidified melt must exist in close contact with the Fe-enriched sphalerite¹⁵. The conditions shown in the experiments may hold true for the formation of CD at Rajpura–Dariba and Ambaji–Deri deposits. Still many other parameters as discussed by Bente and Doering¹⁸, like temperature, time, f_{S_2} , f_{O_2} have a direct influence on the form of CD, the reason for their different FD values. Inhomogeneities of the sphalerite grain also have an important role in shaping the CD form. According to Williams⁴⁹, the rate of diffusion is more rapid along the irregular part of the crystal like the twin boundaries. Thus CD texture formed in the monocrystalline part would be different than the one in the fractures, as also supported by Bente and Doering¹⁷. Barton and Bethke⁷ observed that within the same sample diffusion can be much rapid in some circumstances than others, thus affecting the initial form of CD. Also, the availability of Cu and Fe is key for the nucleation of chalcopyrite and its initial shape that may change according to the nature of metamorphic events. Possibly additional fractal data of CD from other deposits that witnessed different grades of metamorphism may shed more light on whether there exists a correlation between FD and metamorphic grade.

Conclusion

In this limited study we have been able to identify the fractal nature of CD, and verify the experimental results on a wide range of forms of CD. A positive correlation is noted between FD and the peak metamorphic grade of the studied deposits. Quantifying a texture has always been challenging, and the present study shows the importance of using fractals as a useful tool to explain the patterns produced by geological processes that may be self-similar. We hope these data would encourage more detailed study of CD at the atomic level through modern tools like AFM, neutron scattering and further mathematical simulation of CD that could reveal more information about its fractal nature and a better quantification of this texture.

1. Betekhtin, A. G., Genkin, A. D., Filimonova, A. A. and Shadlun, T. N., *Structures and Textures of Ores*, Gosgeoltekhisdat, Moscow, Russia, 1958, p. 435.
2. Grigoriev, I. F., Textures of mineral intergrowths in ores. *Zap. Vses. Mineral. Ova.*, 1928, **57**, 11–56.
3. Ramdohr, P., Beobachtungen an opaken Erzen. *Arch. Lagerstaettenforsch.*, 1924, **34**, 30.
4. Schneiderhöhn, H., Anleitung zur microscopischen Bestimmung und Untersuchung von Erzen und Aufbereitungsprodukten, besonderes im auffallenden Licht: Berlin, Selbstverlag Gesell. Deutsche Metallhiitten Bergleute, 1922, p. 292.
5. Nakano, N., On the microscopic intergrowths of chalcopyrite and zincblende. *Jpn. Assoc. Mineral. Petrol. Econ. Geol. J.*, 1937, **18**, 23–29.
6. Barton, P. B., Some ore textures involving sphalerite from the Furutobe mine, Akita Prefecture, Japan. *Min. Geol.*, 1978, **28**, 293–300.
7. Barton, P. B. and Bethke, P. M., Chalcopyrite disease in sphalerite: pathology and epidemiology. *Am. Mineral.*, 1987, **76**, 451–467.
8. Sugaki, A., Kitakaze, A. and Kojima, S., Bulk compositions of intimate intergrowths of chalcopyrite and sphalerite and their genetic implications. *Miner. Deposita*, 1987, **22**(1), 26–32.
9. Eldridge, C. S., Bourcier, W. L., Ohmoto, H. and Barnes, H. L., Hydrothermal inoculation and incubation of the chalcopyrite disease in sphalerite. *Econ. Geol.*, 1988, **83**(5), 978–989.
10. Wiggins, L. B. and Craig, J. R., Reconnaissance of the Cu–Fe–Zn–S system; sphalerite phase relationships. *Econ. Geol.*, 1980, **75**(5), 742–751.
11. Mizuta, T., Interdiffusion rate of zinc and iron in natural sphalerite. *Econ. Geol.*, 1988, **83**, 1205–1220.
12. Kojima, S., A co-precipitation experiment on intimate association of sphalerite and chalcopyrite and its bearing on the genesis of Kuroko ores. *Min. Geol.*, 1990, **40**, 147–158.
13. Hutchinson, M. N. and Scott, S. D., Sphalerite geobarometry in the system Cu–Fe–Zn–S. *Econ. Geol.*, 1981, **76**, 143–155.
14. Kojima, S. and Sugaki, A., Phase relations in the Cu–Fe–Zn–S system between 500 and 300 under hydrothermal conditions. *Econ. Geol.*, 1985, **80**, 158–171.
15. Govindarao, B., Pruseth, K. L. and Mishra, B., Sulfide partial melting and chalcopyrite disease: an experimental study. *Am. Mineral.*, 2018, **103**(8), 1200–1207.
16. Pruseth, K. L., Mishra, B., Jehan, N. and Kumar, B., Evidence of sulfide melting and melt fractionation during amphibolite facies metamorphism of the Rajpura–Dariba polymetallic sulfide ores. *Ore Geol. Rev.*, 2016, **72**, 1213–1223.
17. Bente, K. and Doering, T., Solid state diffusion studies in sphalerite: an experimental verification of the ‘chalcopyrite disease’. *Eur. J. Mineral.*, 1993, **53**, 285–305.
18. Bente, K. and Doering, T., Experimental studies on the solid state diffusion of (Cu + In) in (ZnS) and on ‘disease’, DIS (diffusion induced segregations), in sphalerite and their geological application. *J. Mineral. Petrol.*, 1995, **53**, 285–305.
19. Mandelbrot, B. B., *The Fractal Geometry of Nature* (revised and enlarged edition), Freeman and Co, NY, USA, 1983, p. 495.
20. Lipowsky, R., Scaling properties of interfaces and membranes. In *Random Fluctuations and Pattern Growth: Experiments and Models*, Springer, The Netherlands, 1988, pp. 227–245.
21. Agterberg, F. P., Bonham-Carter, G. F., Cheng, Q. and Wrigh, D. F., Weights of evidence modeling and weighted logistic regression for mineral potential mapping. In *Computers in Geology – 25 years of Progress*, Oxford University Press, NY, USA, 1993, pp. 13–32.
22. Ford, A. and Blenkinsop, T. G., Combining fractal analysis of mineral deposit clustering with weights of evidence to evaluate patterns of mineralization: application to copper deposits of the Mount Isa Inlier, NW Queensland, Australia. *Ore Geol. Rev.*, 2008, **33**(3–4), 435–450.
23. Changjiang, L., Youlang, X. and Xuliang, J., *Fractal Nature of Mineral Deposit*, Geology of Zhejiang, 2, 1994.
24. Blenkinsop, T. G., Kruhl, J. H. and Kupková, M. (eds), *Fractals and Dynamic Systems in Geoscience*, Birkhäuser Verlag, Basel, Switzerland, 2000.
25. Gulbin, Y. L. and Evangulova, E. B., Morphometry of quartz aggregates in granites: fractal images referring to nucleation and growth processes. *Math. Geol.*, 2003, **35**(7), 819–833.
26. Huber, M. A., Dynamics of metamorphism processes by the fractal textures analysis of garnets, amphiboles and pyroxenes of Lapland Granulite Belt, Kola Peninsula. *J. Biol. Earth Sci.*, 2012, **2**(2), 50–55.
27. Nkono, C., Féménias, O., Lesne, A., Mercier, J. C., Ngounouno, F. Y. and Demaiffe, D., Relationship between the fractal dimension of orthopyroxene distribution and the temperature in mantle xenoliths. *Geol. J.*, 2016, **51**(5), 748–759.
28. Kueppers, U., Scheu, B., Spieler, O. and Dingwell, D. B., Fragmentation efficiency of explosive volcanic eruptions: a study of experimentally generated pyroclasts. *J. Volcanol. Geotherm. Res.*, 2006, **153**, 125–135.
29. Bindeman, I. N., Fragmentation phenomena in populations of magmatic crystals. *Am. Mineral.*, 2005, **90**, 1801–1815.
30. Yu, C. and Liu, J., Fractal and multifractal analyses of sphalerite banding at the Zhaishang gold deposit, western Qinling, China. *Eur. J. Mineral.*, 2015, **27**, 511–520.
31. Fowler, A. D. and L’Heureux, I., Self-organized banded sphalerite and branching galena in the Pine Point ore deposit, Northwest Territories. *Canadian Mineral.*, 1996, **34**(6), 1211–1222.
32. Xia, F. *et al.*, A characterization of porosity in sulfide ore minerals: a USANS/SANS study. *Am. Mineral.*, 2014, **99**, 2398–2404.
33. Heron, A. M., The geology of central Rajputana. *Mem. Geol. Surv. India*, 1953, **79**, 389.
34. Deb, M., Genesis and metamorphism of two stratiform massive sulphide deposits at Ambaji and Deri in the Precambrian of western India. *Econ. Geol.*, 1980, **75**, 572–591.
35. Deb, M. and Sarkar, S. C., Proterozoic tectonic evolution and metallogenesis in the Aravalli–Delhi orogenic complex, northwestern India. *Precambrian Res.*, 1990, **46**, 115–137.
36. Raghunandan, K. R., Dhruva Rao, B. K. and Singhal, M. L., Exploration for copper, lead and zinc ores in India. *Bull. Geol. Surv. India, Ser. A*, 1981, **47**, 16–18.
37. Tripathi, S., Geological characterisation of the carbonate-hosted polymetallic prospect at Imalia, Mahakoshal belt, Central India. Unpublished PhD thesis, University of Delhi, India, 2008, p. 315.
38. Peternell, M. and Kruhl, H., Automation of pattern recognition and fractal-geometry-based pattern quantification, exemplified by

- mineral-phase distribution patterns in igneous rocks. *Comput. Geosci.*, 2011, **35**, 1415–1426.
39. Pruess, S. A., Some remarks on the numerical estimation of fractal dimension. In *Fractals in the Earth Sciences* (eds Barton, C. C. and La Pointe, P. R.), Plenum Press, NY, USA, 1995, pp. 65–76.
40. Deb, M., Polymetamorphism of ores in Precambrian stratiform massive sulfide Deposits at Ambaji–Deri, Western India. *Miner. Deposita*, 1979, **14**, 21–31.
41. Tiwary, A., Deb, M. and Cook, N. J., Use of pyrite microfabric as a key to tectono-thermal evolution of massive sulphide deposits – an example from Deri, southern Rajasthan, India. *Mineral. Mag.*, 1998, **62**(2), 197–212.
42. Li, J. M., Lü, L., Lai, M. O. and Ralph, B., *Image Based Fractal Description of Microstructures*, 2003, Kluwer, p. 272.
43. Deb, M. and Bhattacharya, A. K., Geological setting and conditions of metamorphism of Rajpura–Dariba polymetallic ore deposit, Rajasthan, India. In Proceedings of the 5th IAGOD symposium, Schweizerbart'sche Verlagsbuchhandlung, Stuttgart, Germany, 1980, pp. 679–697.
44. Pal, T., Ore deposit modeling in the Dariba–Rajpura–Bethumni belt, Rajasthan, in the light of a database on sediment-hosted Pb–Zn sulphide deposits in India, 2006, Unpublished Ph D thesis, p. 311.
45. Mishra, B. Evolution of the Rajpura–Dariba polymetallic sulphide deposit: constraints from sulphide–sulfosalt phase equilibria and fluid inclusion studies. In *Crustal Evolution and Metallogeny in the Northwestern Indian Shield*, Narosa Publication, New Delhi, 2000, pp. 347–370.
46. Mishra, B., Upadhyay, D. and Bernhardt, H.-J. Metamorphism of the host and associated rocks at the Rajpura–Dariba massive sulfide deposit, Northwestern India. *J. Asian Earth Sci.*, 2006, **26**(1), 21–37.
47. Bortnikov, N. S., Genkin, A. D., Dobrovolskaya, M. G., Muravitskaya, G. N. and Filimonova, A. A., The nature of chalcopyrite inclusions in sphalerite: exsolution, coprecipitation, or 'disease'? *Econ. Geol.*, 1991, **86**, 1070–1082.
48. Nagase, T. and Kojima, S., An SEM examination of the chalcopyrite disease texture and its genetic implications. *Mineral. Mag.*, 1997, **61**, 89–97.
49. Williams, V. A., Diffusion of some impurities in zinc sulphide single crystals. *J. Mater. Sci.*, 1972, **7**(7), 807–812.

ACKNOWLEDGEMENT. We thank Prof. M. Deb, University of Delhi for providing the samples of Ambaji–Deri deposit and for reviewing the manuscript.

Received 17 December 2018; revised accepted 23 April 2019

doi: 10.18520/cs/v117/i3/460-469